

**CONNECTIVE HEAT AND MASS TRANSFER FLOW OF A ROTATING FLUID  
IN A VERTICAL CHANNEL BOUNDED BY STRETCHING AND STATIONARY WALLS  
WITH SORET EFFECT, THERMAL RADIATION, CHEMICAL REACTION  
IN PRESENCE OF NON-UNIFORM HEAT SOURCES**

**J. S. SUKANYA\*<sup>1</sup> AND Prof. A. LEELA RATHNAM<sup>2</sup>**

**<sup>1</sup>Research scholar in Applied Mathematics,  
Sri Padmavathi Mahila University, Tirupati (A.P.), India.**

**<sup>2</sup>Professor, Applied Mathematics,  
Sri Padmavathi Mahila University, Tirupati (A.P.), India.**

**(Received On: 23-07-18; Revised & Accepted On: 01-09-18)**

---

**ABSTRACT**

*In this paper, we investigate the solet effect, thermal radiation, chemical reaction on convective heat and mass transfer flow of an electrically conducting, viscous, incompressible rotating fluid in a vertical channel bounded by stretching sheet and stationary walls in presence of non-uniform heat sources. The non-linear governing equations have been solved by using Runge-Kutta shooting technique. The velocity, temperature and concentration have been analysed for different variations of  $N_r$ ,  $R$ ,  $Ec$ ,  $Al$ ,  $B1$  and  $Sr$ . The rate of Skin friction, rate of heat and mass transfer are evaluated numerically for different variations.*

**Keywords:** Heat and Mass Transfer, Stretching walls, Constant Heat and Flux and Mass Flux.

---

**1. INTRODUCTION**

Laminar flows through channels have applications in the fields of gas diffusion, ablation cooling, filtration, micro fluidic devices, surface sublimation, grain regression(as in the case of combustion in rocket motors) and the modelling of air circulation in the respiratory system(10).Laminar air –flow systems have been used by the aerospace industry to control particular contamination. Futhermore, the laminar flow cabinet have been used in the maintenance of negative pressure and in the adjustment of the fans to exhaust more air. Therefore, the Navier-Stokes equations which are the governing equations for these problems have attracted the interest of the researchers. Sutton and Barto [21] described an exact solution of Navier-Stokes equations for motion of an incompressible viscous fluid in a channel with different pressure gradients. Their solutions are helpful in verifying and validating computational models of complex on unsteady motions, to guide the design of fuel injectors and controlled experiments. Simulation of flow through microchannels with design roughness was presented numerically by Rawool *et.al* [19] A numerical investigations is made by Robinson [18] for the problem of steady laminar incompressible flow in a porous channel with uniform suction at both walls. Taylor *et.al* [24] studied thress dimensional flow buy uniform suction through parallel porous walls. The investigations of Taylor [24] were further extended to a more general three dimensional stagnation point which can capture the phenomena in a single class of state by Hewitt *et.al* [8].Two dimensional viscous incompressible fluid flow between two porous walls with uniform suction was analysed by Cox [5]. Berman [3] proposed the two dimensional laminar steady flow through a porous channel which was driven by suction or injection .Similarity one/two dimensional laminar flow in a porous channel with wall suction or injection was examined analytically by Laurent *et.al* [11]. The problem of fluid flow in a channel with porous walls was solved by Karode [9]. Zheng *et.al* [29] investigated asymptotic solutions for steady laminar flow of an incompressible viscous fluid along a channel with accelerating rigid porous walls. The exact solution solution for two dimensional steady laminar flow through a porous channel was generalized by Terril [13], Shrestil and Terril [22, 25], Brady [4], Waston *et.al* [27] and Cox [5] under varied conditions. Deng and Martinez [19] worked on two dimensional flow of a viscous fluid in a channel partially filled with porous medium with wall suction. Wang [26] worked on viscous flow due to stretching sheet with slip and suction and proved a closed form unique solution for two dimensiunal flows. For axisymmetric stretching both

---

**Corresponding Author: J. S. Sukanya\*<sup>1</sup>, <sup>1</sup>Research scholar in Applied Mathematics,  
Sri Padmavathi Mahila University, Tirupati (A.P.), India.**

existence and uniqueness were shown. Muhammad Ashraf *et.al* [14] investigated micropolar fluid flow in a channel with Shrinking walls. Hajipour and Dehkordi [7] studied the transient behaviour of fluid flow and heat transfer in vertical channel partially filled with a porous medium including the effects of inertial term and viscous dissipation. Kashif Ali *et.al* [10\*] have discussed numerical study of micropolar fluid flow and heat transfer in a channel with shrinking and stationary wall. Pudi Sreenivasa Rao [15] has discussed the effect of chemical reaction and dissipation on MHD convective heat and mass transfer flow in a vertical channel bounded by stretching and stationary walls in the presence of heat sources. Madhavi *et.al* [12] have investigated heat and mass transfer flow of a rotating fluid in a vertical channel with stretching and stationary walls.

## 2. FORMULATION OF THE PROBLEM

We consider the steady two dimensional hydromagnetic laminar convective heat and mass transfer flow of a viscous electrically conducting fluid through a porous medium in a vertical channel bounded by a stretching plate on the left and a stationary plate on the right. We choose a rectangular coordinate system O(x, y,z) with the walls at  $y=\pm L$ . The flow is subjected to a strong magnetic field with a constant intensity  $B_0$  along the positive y-direction. Assuming magnetic Reynolds number  $R_m$  to be small we neglect the induced magnetic field in comparison to the applied magnetic field. It is used to compare the transport of magnetic lines of the force in a conducting fluid with the leakage of such lines from the fluid.

Taking the viscous dissipation and joule heating effects into consideration, the governing equations of the flow, heat and mass transfer with Roseland approximation for the radiative heat flux are given by

$$\frac{\partial u}{\partial x} + \frac{\partial v}{\partial y} = 0 \quad (1)$$

$$\rho \left( u \frac{\partial u}{\partial x} + v \frac{\partial u}{\partial y} \right) = -\frac{\partial p}{\partial x} + \mu \left( \frac{\partial^2 u}{\partial x^2} + \frac{\partial^2 u}{\partial y^2} \right) - \sigma \mu_e^2 H_o^2 - \rho g + 2\Omega w \quad (2)$$

$$\rho \left( u \frac{\partial v}{\partial x} + v \frac{\partial v}{\partial y} \right) = -\frac{\partial p}{\partial y} + \mu \left( \frac{\partial^2 v}{\partial x^2} + \frac{\partial^2 v}{\partial y^2} \right) \quad (3)$$

$$\rho \left( u \frac{\partial w}{\partial x} + v \frac{\partial w}{\partial y} \right) = \mu \left( \frac{\partial^2 w}{\partial x^2} + \frac{\partial^2 w}{\partial y^2} \right) - \sigma \mu_e^2 H_o^2 - 2\Omega u \quad (4)$$

$$\begin{aligned} \rho C_p \left( u \frac{\partial T}{\partial x} + v \frac{\partial T}{\partial y} \right) &= k_f \left( \frac{\partial^2 T}{\partial x^2} + \frac{\partial^2 T}{\partial y^2} \right) + q''' + \frac{16\sigma^* T_\infty^3}{3\beta_R} \frac{\partial^2 T}{\partial y^2} \\ &+ 2\mu \left( \left( \frac{\partial u}{\partial y} \right)^2 + \left( \frac{\partial w}{\partial y} \right)^2 \right) + \sigma \mu_e^2 H_o^2 (u^2 + w^2) \end{aligned} \quad (5)$$

$$\left( u \frac{\partial C}{\partial x} + v \frac{\partial C}{\partial y} \right) = D_b \left( \frac{\partial^2 C}{\partial x^2} + \frac{\partial^2 C}{\partial y^2} \right) - k'_c (C - C_o) + \frac{D_T K_T}{T_m} \left( \frac{\partial^2 T}{\partial x^2} + \frac{\partial^2 T}{\partial y^2} \right) \quad (6)$$

$$\rho - \rho_o = -\beta(T - T_o) - \beta^*(C - C_o) \quad (7)$$

Where(u,v,0) are the velocity components along x, y directions respectively, T, C are the dimensional temperature and concentration respectively,  $\rho$  is the density, p is the pressure,  $\sigma$  is the electrical conductivity,  $\mu_e$  is the magnetic permeability of the medium,  $\mu$  is the dynamic viscosity, g is the gravity, is the strength of the heat source,  $D_b$  is the molecular diffusivity,  $D_T$  is the mass diffusivity,  $K_T$  is the thermal diffusion ratio,  $\beta$  is the coefficient of thermal expansion,  $\beta^*$  is the coefficient of volume expansion,  $T_m$  is the mean fluid temperature.

The coefficient  $q'''$  is the rate of internal heat generation ( $>0$ ) or absorption ( $<0$ ). The internal heat generation /absorption  $q'''$  is modelled as

$$q''' = \left( \frac{ku_s}{xv} \right) [A1(T_1 - T_1)f'(\eta) + B1(T - T_2)] \quad (8)$$

Where A1 and B1 are coefficients of space dependent and temperature dependent internal heat generation or absorption respectively. It is noted that the case  $A1>0$  and  $B1>0$ , corresponds to internal heat generation and that  $A1<0$  and  $B1<0$ , the case corresponds to internal heat absorption case.

The boundary conditions for the velocity, temperature and concentration are

$$\begin{aligned} u(x, -L) = us = bx, u(x, +L) = 0, v(x, \pm L) = 0, \\ T(x, -L) = T_1, T(x, +L) = T_2 \\ C(x, -L) = C_1, C(x, +L) = C_2 \end{aligned} \quad (9)$$

Where  $b > 0$  is the stretching rate of the channel wall,  $T_1, T_2$  (with  $T_1 > T_2$ ) are the fixed temperature of the left and right walls respectively,  $C_1, C_2$  (with  $C_1 > C_2$ ) or the fixed concentrations of the channel walls respectively. We introduce the following Similarity variables as:

$$\begin{aligned} \eta = \frac{y}{L}; u = bxf'(\eta); v = -bLf(\eta), w = bxg_0(\eta) \\ \theta(\eta) = \frac{T - T_2}{T_1 - T_2}, \phi(\eta) = \frac{C - C_2}{C_1 - C_2} \end{aligned} \quad (10)$$

The above velocity field is compatible with continuity equation (1) and therefore, represents the possible fluid motion.

Eliminating the pressure between the equations (2) and (3) and using (6) & (8) the momentum equation reduces to

$$f^{iv} + \text{Re}_x(f f'' - f' f') - M^2 f'' + Gr(\theta' + N\phi') + Rg_0' = 0 \quad (11)$$

$$g_0^{ii} + \text{Re}_x(f_0 g' - f' g_0) - M^2 g_0 - Rf' = 0 \quad (12)$$

where as the equations (5) & (6) in view of equation (9).are

$$\left(1 + \frac{4Nr}{3}\right) \theta'' + \text{Pr Re}_x(f \theta') + (A_1 f' + B_1 \theta) + \text{Pr Ec}((f'')^2 + (g_0')^2) + \frac{M^2 Ec}{1 + m^2}((f')^2 + g_0^2) = 0 \quad (13)$$

$$\phi'' + \text{Sc Re}_x(f \phi') - \gamma \phi + (Sc Sr) \theta'' = 0 \quad (14)$$

where  $Gr = \frac{\beta g(T_1 - T_2)L}{bx}$ , is the Grashof number,  $N = \frac{\beta^*(C_1 - C_2)}{\beta(T_1 - T_2)}$ , is the buoyancy ratio,

$M^2 = \frac{\sigma \mu_e^2 H_o^2 L^2}{\nu x}$ , magnetic parameter,  $D^{-1} = \frac{L^2}{k}$ , Inverse Darcy parameter,

$\text{Pr} = \frac{\mu C_p}{k_f}$  is Prandtl number,  $\text{Re}_x = \frac{bL^2}{\mu}$ , is the local Reynolds number,

$Sc = \frac{\nu}{D_m}$ , is the Schmidt number,  $S_r = \frac{D_r K_r (T_1 - T_2)}{T_m (C_1 - C_2)}$ , is the Soret parameter

$\gamma = \frac{k_c L^2}{D_m}$  is the chemical reaction parameter,  $Ec = \frac{b^2 x^2}{C_p \Delta T}$  is the Eckert number,

$R = \frac{2\Omega}{xL}$  Rotation Parameter

Boundary conditions (9), in view of equation (10) in dimensional form reduces to

$$\begin{aligned} f(\pm 1) = 0, f'(-1) = 1, f'(1) = 0, g_0(-1) = 0, g_0(1) = 0 \\ \theta(-1) = 1, \theta(1) = 0, \phi(-1) = 1, \phi(1) = 0, \end{aligned} \quad (15)$$

### 3. METHOD OF SOLUTION

A usual approach is to write the nonlinear ODE in form of a a first order initial value problem as follows:

$$f = f_1, f' = f_2, f'' = f_3, f''' = f_4, g = f_5, g' = f_6 \quad (16)$$

$$\theta = f_7, \theta' = f_8, \phi = f_9, \phi' = f_{10}$$

$$f^{iv} = f_4' = -\text{Re}_x(f_4 f_1 - f_2 f_3) - M^2 f_3 - Rf_6 + Gr(f_6 + Nf_8) \quad (17)$$

$$g^{ii} = f_6' = -\text{Re}_x(f_6 f_1 - f_2 f_5) - M^2 g + Rf_2 \quad (18)$$

$$\theta'' = f_8' = [-\text{Pr Re}_x(f_1 f_6) + (A_1 f_2 + B_1 f_7) - \text{Pr Ec}(f_3^2 + f_6^2) - M^2 Ec(f_2^2 + f_5^2)] \quad (19)$$

$$\phi'' = f_8' = [-Sc Re_x(f_1 f_{10}) + \gamma f_9 - Sc So(-Pr Re_x(f_1 f_8) - (A1 f_2 + B1 f_7) - \frac{M^2 Ec}{1+m^2}(f_2^2 + f_5^2) - Pr Ec(f_3^2 + f_5^2)] / (1 + Sc Sr) \quad (20)$$

The corresponding boundary conditions are

$$\begin{aligned} f_1(\pm 1) &= 0, f_2(-1) = 1, f_2(+1) = 0, f_5(-1) = 1, f_5(+1) = 0, \\ f_6(-1) &= 1, f_6(+1) = 0, f_7(-1) = 1, \\ f_7(+1) &= 0, f_8(-1) = 1, f_8(+1) = 0, \end{aligned} \quad (21)$$

Here  $f_3(-1), f_4(-1), f_6(-1), f_8(-1), f_{10}(-1)$  are the unknown initial condition, Therefore, a shooting methodology is incorporated to solve the above system, which may be a combination of the Runge-Kutta method (to solve first order ODE) and a five dimensional zero finding algorithm(to find the missing coordinates).It is note that the missing initial conditions are coupled so that the solution satisfies the boundary conditions

$f(+1) = 0, f'(+1) = 0, g(+1) = 0, \theta(+1) = 0, \phi(+1) = 0$  of the original boundary value problem.

#### 4. DISCUSSION OF NUMERICAL RESULTS

In this analysis we investigate the influence of rotation, thermal radiation, thermo-diffusion and non-uniform heat sources, chemical reaction on non-linear convective heat and mass transfer flow of a viscous, dissipative fluid in a vertical channel bounded by a stretching sheet and stationary plates. The non-linear governing equations have been solved by employing Fourth order Runge-Kutta –Shooting technique.

The primary velocity, secondary velocity, temperature and concentration have been analysed for different variations of R, Nr, A1, B1, Ec and Sr.

Figs.1a-1d represent the variation of f, g,  $\theta$ ,  $\phi$  with radiation parameter Nr. It can be seen from the profiles that both the velocity components, and the concentration reduces and the temperature increases with increase in radiation parameter Nr. This can be attributed to the fact increase in Nr reduces the thickness of the momentum and solutal boundary layers and increases the thermal boundary layer.

The effect of dissipation (Ec) on f, g,  $\theta$  and C is shown in figs. 2a-2d. It can be found that higher the dissipative energy larger the magnitude of the velocity components, temperature and smaller the concentration in the flow region. This is due to the fact that heat energy is reserved due to frictional heating (figs.2a-2d).

Figs.3a-3d, illustrates f, g,  $\theta$ ,  $\phi$  with variation in space dependent Heat source parameter ( $A1 > 0$ ). The presence of the heat sources generates energy in the momentum boundary layer, thermal boundary layer and in solutal boundary layer the energy is absorbed and as a consequence the velocity components, temperature increase and the concentration reduces in the boundary layers. In the case of heat absorption ( $A1 < 0$ ) the velocity components, temperature reduces and the concentration rises with decreasing values of  $A1 < 0$ , owing to the absorption of energy in the boundary layer.

Figs.4a-4d, illustrates  $f^*$ , g,  $\theta$ ,  $\phi$  with variation in temperature dependent heat source parameter ( $B1 > 0$ ). As in the case of space dependent heat source, the velocity components, temperature enhances and the concentration decrease due to the release of energy for  $B1 > 0$  while they drop for decreasing values of  $B1 < 0$  owing to the absorption of energy. The presence of the temperature dependent heat sources generates energy in the momentum boundary layer, thermal boundary layer and absorbed in the solutal boundary layer and as a consequence the velocity components, temperature increases and the concentration enhances in the boundary layers. In the case of heat absorption ( $B1 < 0$ ) the velocity components, temperature reduces and the concentration rises with decreasing values of  $B1 < 0$ , owing to the absorption of energy in the boundary layer.

The effect of rotation parameter (R) on  $f^*$ , g,  $\theta$ ,  $\phi$  is demonstrated in figs.5a-5d. We observe from the profiles that the both the velocity components reduces and the temperature, concentration increases with increase in R in the entire flow region. Thus higher the coriolis force smaller the thickness of the momentum boundary layer and larger the thermal and solutal boundary layers.

Figs.6a-6d represent  $f^*$ , g,  $\theta$  and C with Soret parameter Sr. It can be noticed from the profiles that higher the thermo-diffusion effects larger the magnitude of velocity components, temperature and concentration in the flow region. This can be attributed to the fact that increasing values of So increases the thickness of the momentum boundary layer, thermal boundary layer and solutal boundary layer.

The variation of skin friction components with radiation parameter  $Nr$  shows that  $(\tau_x)$  reduces at  $\eta=-1$  and increases at  $\eta=+1$  while  $(\tau_z)$  increases with increase in  $Nr$  at both the walls. With reference to rotation parameter  $R$ , we find that higher the rotation parameter larger the skin friction components at both the walls. With reference to heat source parameter  $A1, B1$  we find that  $(\tau_x)$  reduces at  $\eta=-1$  and enhances at  $\eta=+1$  while,  $(\tau_z)$  enhances at  $\eta=\pm 1$  with increase in the space dependent heat generating source ( $A1>0$ ) while in the heat absorbing heat source.  $(\tau_x)$  enhances at  $\eta=-1$  and reduces at  $\eta=+1$  while  $(\tau_z)$  reduces at both the walls. An increase in the temperature dependent heat source ( $B1>0$ ),  $(\tau_x)$  reduces at  $\eta=-1$  and enhances at  $\eta=+1$  while  $(\tau_z)$  enhances at both the walls while in the case of heat absorbing source,  $(\tau_x)$  enhances at  $\eta=-1$  and reduces at  $\eta=+1$  while  $(\tau_z)$  reduces at  $\eta=\pm 1$  with increase in  $B1<0$ . With increase in  $Ec$ , we notice that  $(\tau_x)$  reduces at  $\eta=-1$  and enhances at  $\eta=+1$  with increase in  $Ec$  while  $(\tau_z)$  increases at both the walls. The variation of Skin friction component with Soret parameter ( $Sr$ ) shows that the skin friction component  $(\tau_x)$  reduces at  $\eta=-1$  and enhances at  $\eta=+1$  with  $Sr$  while,  $(\tau_z)$  increases with  $Sr$  at both the walls.

The rate of heat transfer (Nusselt number) at  $\eta = \pm 1$  is exhibited in tables.1&2 for different parametric variations. An increase in rotation parameter  $R$  reduces  $Nu$  at  $\eta=-1$  and increases it at  $\eta=+1$ . With respect to radiation parameter  $Nr$ , the rate of heat transfer reduces at  $\eta=-1$  and increases at  $\eta=+1$  with increase in radiation parameter  $Nr$ . The rate of heat transfer reduces at  $\eta=-1$  and enhances at  $\eta=+1$  in the space dependent heat generating source ( $A1>0$ ) while in the heat absorbing source,  $Nu$  enhances at  $\eta=-1$  and reduces at  $\eta=+1$ . An increase in  $B1>0$ , reduces  $Nu$  at  $\eta=-1$  and enhances at  $\eta=+1$  while a reversed effect is noticed with increase in  $B1<0$ . Higher the dissipation effects smaller  $Nu$  at  $\eta=-1$  and larger  $Nu$  at  $\eta=+1$ . The variation of  $Nu$  with  $Sr$  shows that higher the thermo-diffusion effects larger  $Nu$  at  $\eta=+1$  and smaller  $Nu$  at  $\eta=-1$ .

The rate of mass transfer (Sherwood number) at  $\eta = \pm 1$  is exhibited in tables.1&2 for different parametric variations. An increase in  $A1>0$  and  $B1>0$  enhances at  $\eta = \pm 1$  while a reversed effect is noticed in behaviour of  $Sh$  with increase in  $A1<0$  and  $B1<0$  at both the walls while an increase  $A1>0$  &  $B1<0$ , increases at  $\eta=-1$  and reduces at  $\eta=+1$ . With respect to  $Nr$  and  $R$  we find that the rate of mass transfer enhances at  $\eta=-1$  and reduces at  $\eta=+1$  fixing the other parameters. Higher the dissipation effects/thermo-diffusion effects larger  $Sh$  at  $\eta = \pm 1$ .

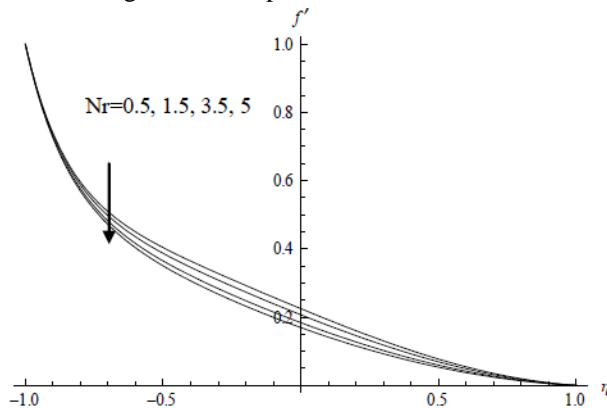


Fig1a. Variation of  $f'$  with  $Nr$   
 $R=0.5, A1=0.1, B1=0.1, Sr=0.5, Ec=0.01$

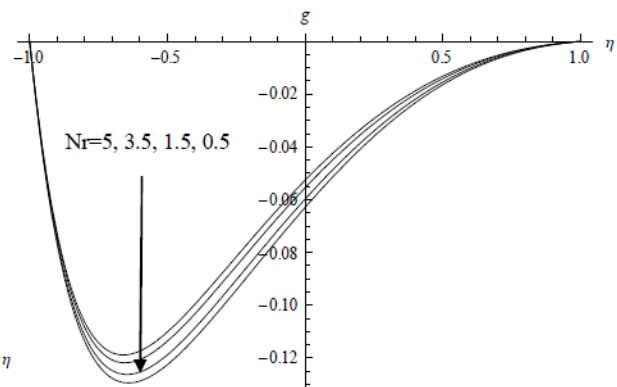


Fig1b. Variation of  $g$  with  $Nr$   
 $R=0.5, A1=0.1, B1=0.1, Sr=0.5, Ec=0.01$

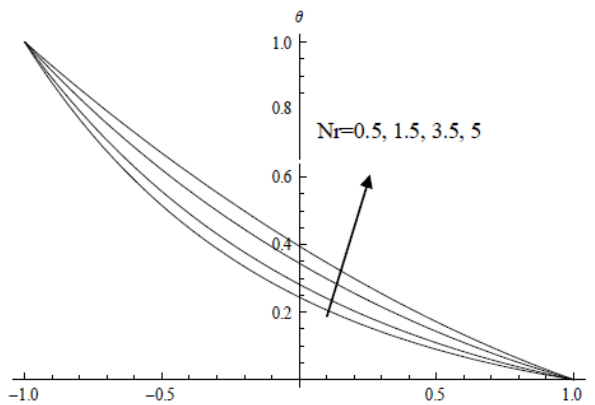


Fig1c. Variation of  $\theta$  with  $Nr$   
 $R=0.5, A1=0.1, B1=0.1, Sr=0.5, Ec=0.01$

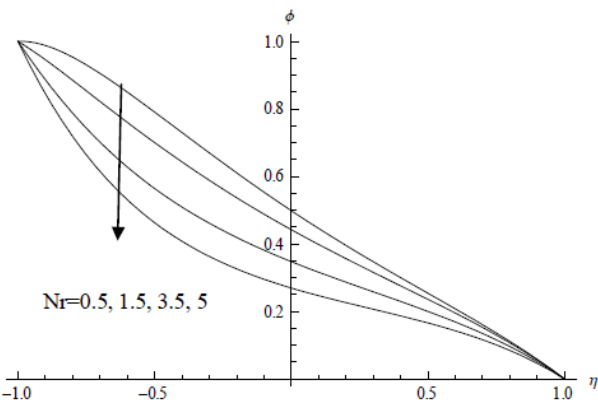


Fig1d. Variation of  $\phi$  with  $Nr$   
 $R=0.5, A1=0.1, B1=0.1, Sr=0.5, Ec=0.01$

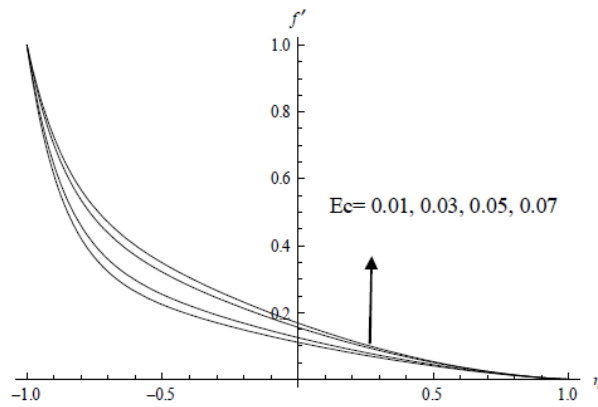


Fig2a. Variation of  $f'$  with  $Ec$   
 $R=0.5, A1=0.1, B1=0.1, Sr=0.5, Nr=0.5$

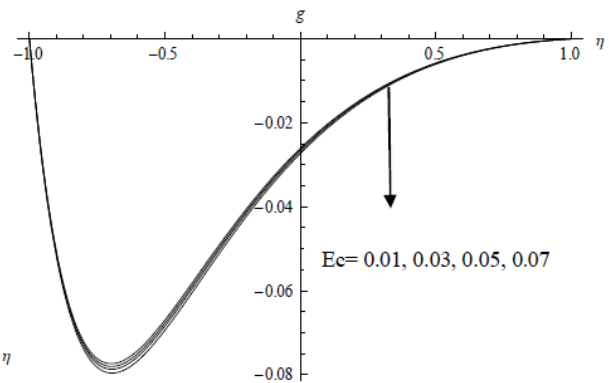


Fig2b. Variation of  $g$  with  $Ec$   
 $R=0.5, A1=0.1, B1=0.1, Sr=0.5, Nr=0.5$

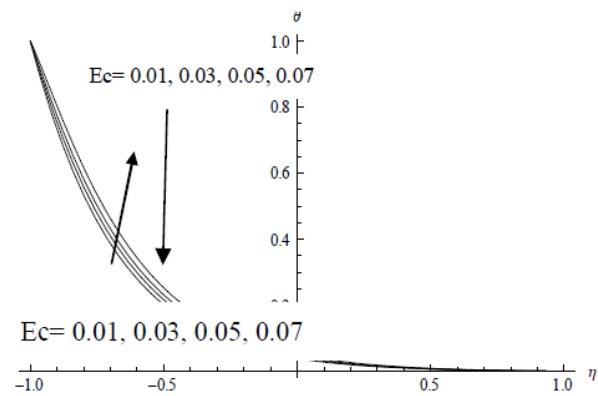


Fig2c. Variation of  $\theta$  with  $Ec$   
 $R=0.5, A1=0.1, B1=0.1, Sr=0.5, Nr=0.5$

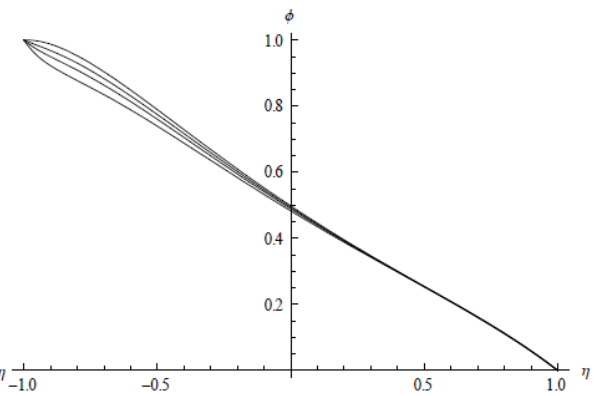


Fig2d. Variation of  $\phi$  with  $Ec$   
 $R=0.5, A1=0.1, B1=0.1, Sr=0.5, Nr=0.5$

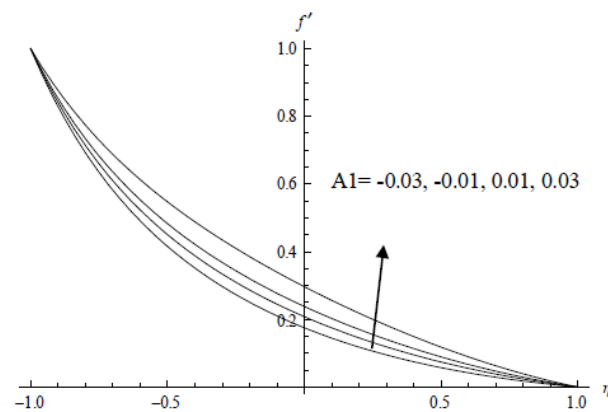


Fig3a. Variation of  $f'$  with  $A1$   
 $R=0.5, Ec=0.01, B1=0.1, Sr=0.5, Nr=0.5$

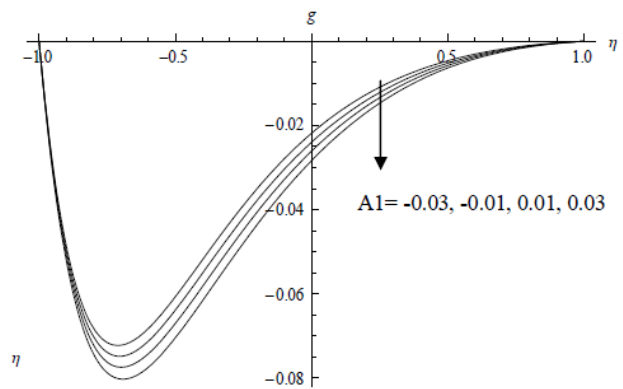


Fig3b. Variation of  $g$  with  $A1$   
 $R=0.5, Ec=0.01, B1=0.1, Sr=0.5, Nr=0.5$

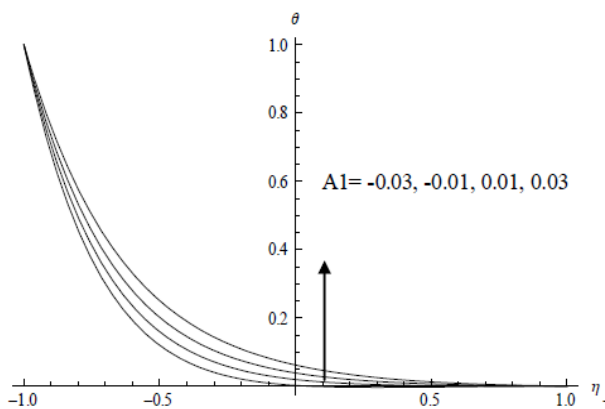


Fig3c. Variation of  $\theta$  with  $A1$   
 $R=0.5, Ec=0.01, B1=0.1, Sr=0.5, Nr=0.5$

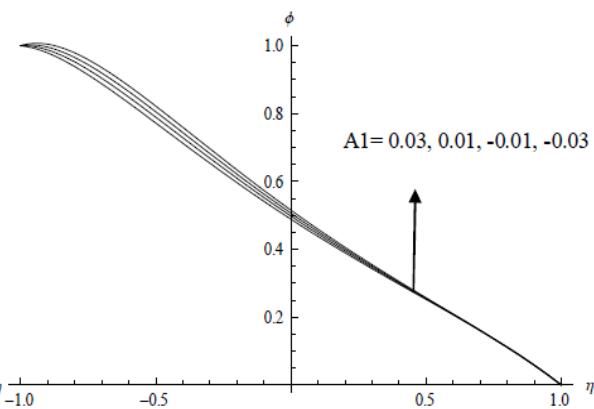


Fig3d. Variation of  $\phi$  with  $A1$   
 $R=0.5, Ec=0.01, B1=0.1, Sr=0.5, Nr=0.5$

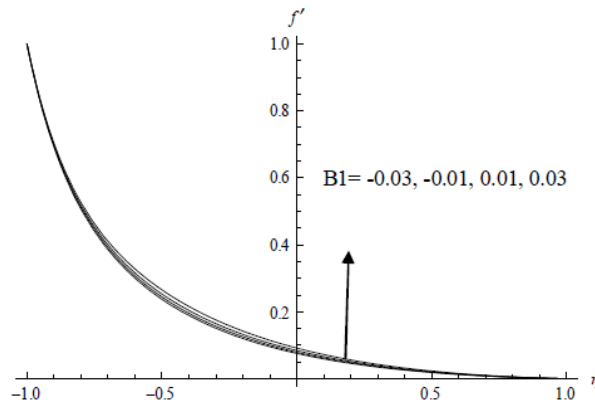


Fig4a. Variation of  $f'$  with  $B1$

$R=0.5, Ec=0.01, A1=0.1, Sr=0.5, Nr=0.5$

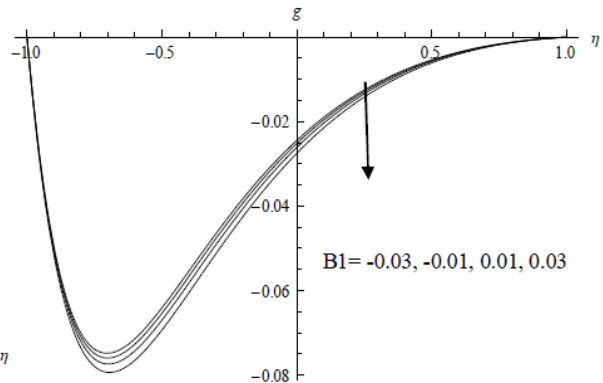


Fig4b. Variation of  $g$  with  $B1$

$R=0.5, Ec=0.01, A1=0.1, Sr=0.5, Nr=0.5$

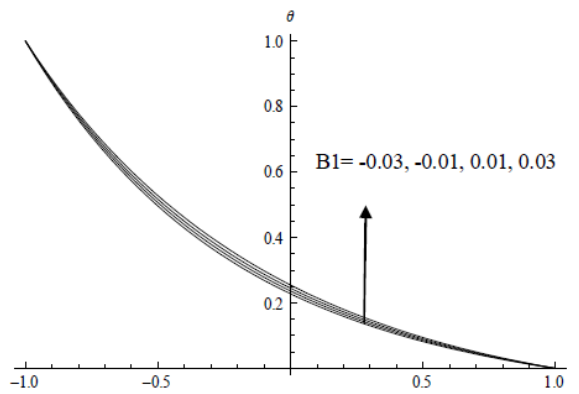


Fig4c. Variation of  $\theta$  with  $B1$

$R=0.5, Ec=0.01, A1=0.1, Sr=0.5, Nr=0.5$

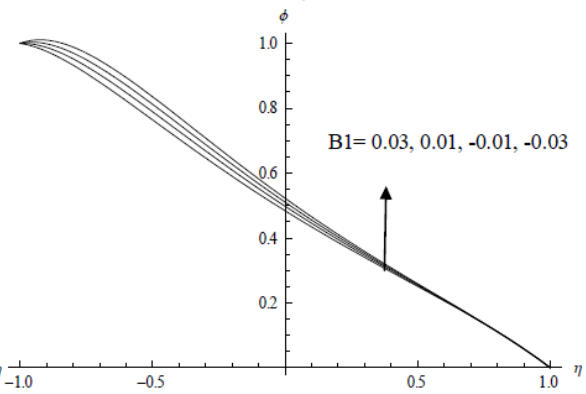


Fig4d. Variation of  $\phi$  with  $B1$

$R=0.5, Ec=0.01, A1=0.1, Sr=0.5, Nr=0.5$

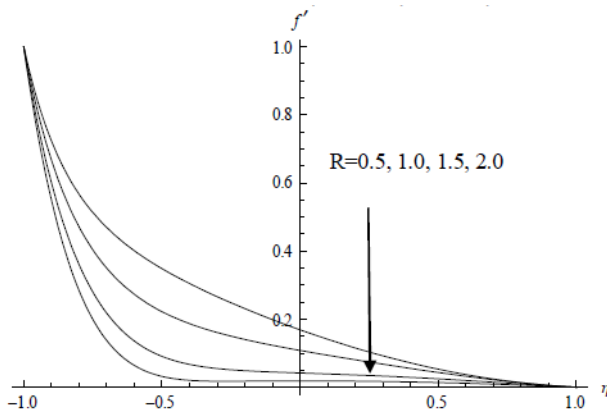


Fig5a. Variation of  $f'$  with  $R$

$B1=0.1, Ec=0.01, A1=0.1, Sr=0.5, Nr=0.5$

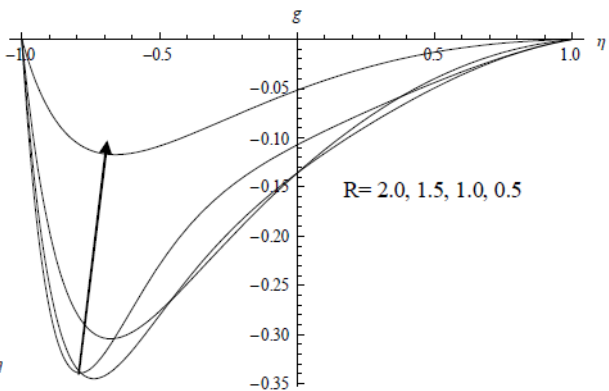


Fig5b. Variation of  $g$  with  $R$

$B1=0.1, Ec=0.01, A1=0.1, Sr=0.5, Nr=0.5$

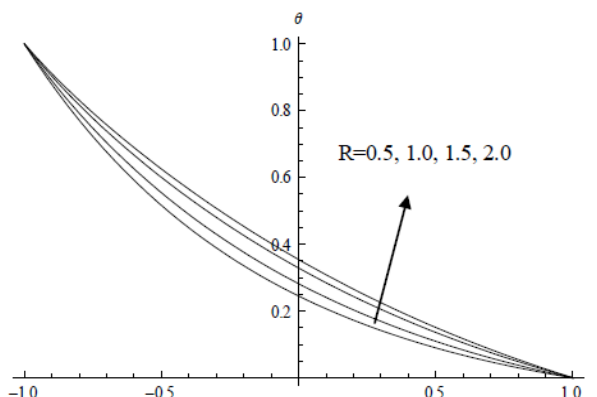


Fig5c. Variation of  $\theta$  with  $R$

$B1=0.1, Ec=0.01, A1=0.1, Sr=0.5, Nr=0.5$

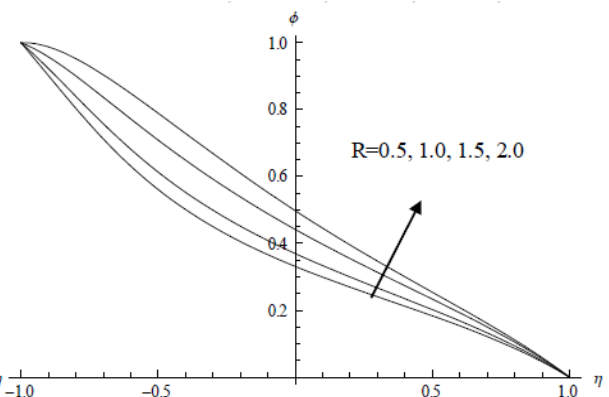


Fig5d. Variation of  $\phi$  with  $R$

$B1=0.1, Ec=0.01, A1=0.1, Sr=0.5, Nr=0.5$



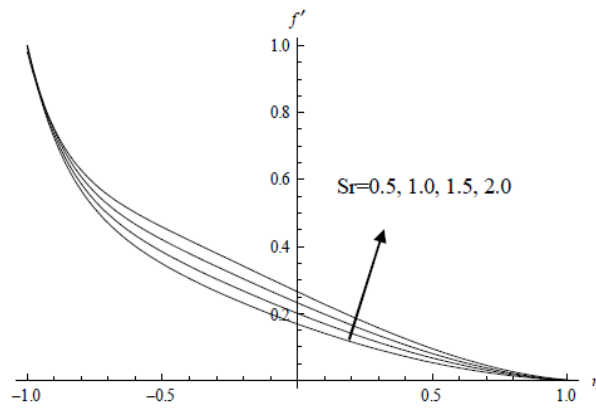


Fig6a. Variation of  $f'$  with  $Sr$   
 $B1=0.1, Ec=0.01, A1=0.1, R=0.5, Nr=0.5$

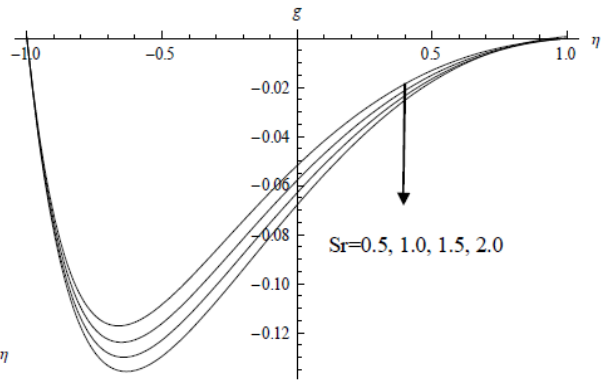


Fig6b. Variation of  $f'$  with  $Sr$   
 $B1=0.1, Ec=0.01, A1=0.1, R=0.5, Nr=0.5$

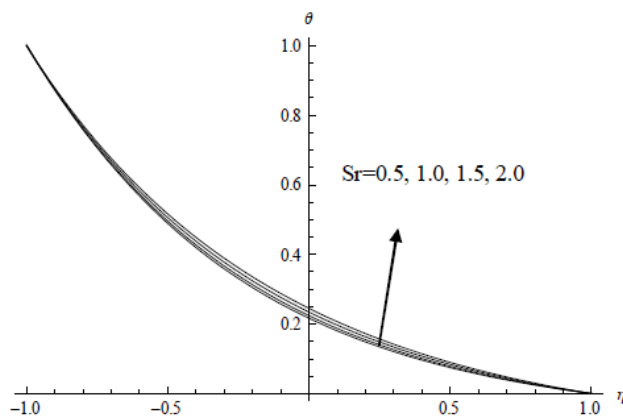


Fig6c. Variation of  $\theta$  with  $Sr$   
 $B1=0.1, Ec=0.01, A1=0.1, R=0.5, Nr=0.5$

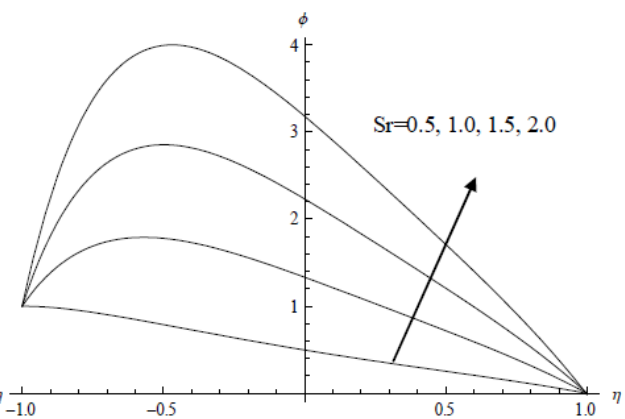


Fig6d. Variation of  $\phi$  with  $Sr$   
 $B1=0.1, Ec=0.01, A1=0.1, R=0.5, Nr=0.5$

**Table-1: Skin friction, Nusselt number and Sherwood number at  $\eta=-1$**

parameters		$\tau_x (-1)$	$\tau_z (-1)$	$Nu(-1)$	$Sh(-1)$
Ec	0.01	-3.7129	-1.00896	1.35677	-0.032609
	0.03	-3.69759	-1.01214	1.13189	0.685716
	0.05	-3.68626	-1.01448	1.00965	1.21637
	0.07	-3.66763	-1.01832	0.80901	2.08667
A1	0.1	-3.7129	-1.00896	1.35677	-0.032609
	0.3	-3.70517	-1.01119	1.26377	-0.079676
	-0.1	-3.72018	-1.00685	1.32882	-0.138909
	-0.3	-3.72775	-1.00465	1.36172	-0.249861
B1	0.1	-3.7129	-1.00896	1.35677	-0.032609
	0.3	-3.70159	-1.01229	1.25182	-0.113901
	-0.1	-3.72326	-1.0059	1.33922	-0.169119
	-0.3	-3.73373	-1.00278	1.38207	-0.309474
Sr	0.5	-3.7129	-1.00896	1.35677	-0.032609
	1.5	-3.68291	-1.01675	1.30467	-1.19533
	2.0	-3.59083	-1.03916	1.27681	-4.79581
	2.5	-3.46356	-1.06693	1.22586	-9.85697
Nr	0.5	-3.63672	-1.03192	1.35677	0.886227
	1.5	-3.55972	-1.05425	0.724277	1.70898
	3.5	-3.47587	-1.0774	0.434858	2.50625
	5.0	-3.35737	-1.10792	0.044538	3.49344
R	0.5	-3.71293	-1.00896	1.35677	0.032609
	1.0	-4.34572	-2.77834	1.17437	0.313647
	1.5	-5.1104	-3.79024	1.02729	0.719465
	2.0	-5.71327	-4.44738	0.94006	0.97336



**Table-2:** Skin friction, Nusselt number and Sherwood number at  $\eta=+1$ 

		$\tau_x (+1)$	$\tau_z (+1)$	Nu(+1)	Sh(+1)
Ec	0.01	-0.0399856	0.00754531	0.064115	0.617247
	0.03	-0.0406445	0.00758389	0.13963	0.624112
	0.05	-0.0411362	0.00761195	0.143238	0.629183
	0.07	-0.0419526	0.00765722	0.149337	0.637498
A1	0.1	-0.0399856	0.00754531	0.064115	0.617247
	0.3	-0.0406049	0.00759567	0.13925	0.620644
	-0.1	-0.0393983	0.0074963	0.130778	0.614079
	-0.3	-0.0387844	0.00744377	0.126552	0.61082
B1	0.1	-0.0399856	0.00754531	0.064115	0.617247
	0.3	-0.0409555	0.00762615	0.14185	0.621059
	-0.1	-0.0390984	0.00746894	0.12862	0.61371
	-0.3	-0.0382035	0.00738957	0.122436	0.610085
Sr	0.5	-0.0399856	0.00754531	0.064115	0.617247
	1.5	-0.042911	0.00779304	0.131989	0.903708
	2.0	-0.0510722	0.00837011	0.143694	1.77443
	2.5	-0.0605972	0.00882416	0.153469	2.95547
Nr	0.5	-0.0479754	0.00819929	0.213075	0.585837
	1.5	-0.056628	0.00877383	0.29034	0.511647
	3.5	-0.0665265	0.00928938	0.410303	0.373097
	5.0	-0.0810246	0.00982241	0.627401	0.0571939
R	0.5	-0.0399856	0.00754531	0.064115	0.617247
	1.0	-0.0430004	0.0294738	0.172854	0.589899
	1.5	-0.0558271	0.0487857	0.226881	0.534751
	2.0	-0.0657045	0.0508484	0.258442	0.496725

## 5. REFERENCES

1. Asia,Y,Kashif,A and Muhammad,A: MHD Unsteady flow and heat transfer of micropolar fluid through porous channel with expanding or contracting walls., JAFM, V.9(4),pp.1807-1817(2016)
2. Ashraf,M,Kamal,M.A and Syed,K.S: Numerical study of asymmetric laminar flow of micropolar fluids in a porous channel .,Computers and fluid., V.38, pp.1895-1902(2009)
3. Berman,A.S: Laminar flow in channels with porous walls., J.Appl.Phys,V.24,pp.1232-1235(1953)
4. Brady,J.F: Flow development in a porous channel and tube, Phys. Fluids, V.27, pp.1061-1067(1984)
5. Cox,S.M:Analysis of steady flow in a channel with one porous wall or with accelerating walls, SIAQM J.Appl.Math, V.51,pp.429-438(1991)
6. Deng,C and Martinez,D.M" Viscous flow in a channel partially filled with a porous medium and with wall suction,Chemical Eng.Sci,V.60, pp.329-336(2005)
7. Hajipour,M and Dehkord,A.M: Transient behaviour of fluid flow and heat transfer in vertical channel partially filled with porous medium:Effects of inertial term and viscous dissipation., Energy Conversion and Management,V.61,pp.1-7(2012)
8. Hewitt,R.E,Duck,P.W and AL-Azhari: Extension to three –dimensional flow in a porous channel., Fluid Dynamics Res., V.33, pp.17-39(2003)
9. Karode,S.K:Laminar flow in channels with porous walls.,Revisited J.Membranes Sci.,V.191, pp.237-241 (2001)
10. Kashif Ali,Muhammad Ashraf: Numerical simulation of the micropolar fluid flow and heat transfer in a channel with a shrinking and stationary wall,J.Theo. and Appl mech.,V.52(2), pp.557-569(2014)
11. Laurent,O,Philippe,S and Michel,Q: Laminar flow in channels with wall suction or injection .,Chemical Eng Sci., V59, pp.1039-1050(2004)
12. Madhavi,S and Prasada Rao,D.R.V: Effect of chemical reaction and thermo-diffusion on convective heat and mass transverse flow of a rotating fluid through a porous medium in a vertical channel with stretching wals., International Journal Maths.Archives., V.8(5), pp.65-79 (2017)
13. Misra,J.C,Shit ,G.C and Rath,H.J: Flow and heat transfer of a MHD viscoelastic fluid in a channel with stretching walls: Some applications to Haemo-dynamics., ZARM, pp.1-26(2010)
14. Muhammad Ashraf and Muhammad Abu Bakar: Micropolar fluid flow in achannel with Shrinking walls,World Appl. sci.J.. V. 115,(8), pp.1074-1081(2011)
15. Pudi Sreenivasa Rao: MHD mixed convective heat and mass transfer in a vertical channel with stretching walls.,Int.Res.and Dev.in Tech.,V.7(4),pp.21-32(2017)
16. Qi,X.G,Scott,D.M and Wilson,D.I:Modelling Laminar pulsed flow in rectangular channel., Eng. sci., V.63, pp.2682-2689(2008).

17. Raftari,B and Vajravelu,K: Homotopy analysis method for MHD viscoelastic fluid flow and heat transfer in a channel with a stretching wall., Commun Nonlinear sci Numer Simulat,V.17, pp.4149-4162 (2012)
18. Robinson,W.A:The existence of multiple solutions for the laminar flow in a uniformly porous channel with suction at both walls.,J.Fluid.Mech.,V,212, pp.451-485(1990)
19. Rawool,A.S Mitra,S.K and Kandilkar, s.G:Numerical simulation of flow through microchannels with designed roughness., Microfluids and Nanofluids.,V.2,pp.215-221(2006)
20. Sarojamma,G, Vasundhara,B and Vendabai, K : MHD Casson fluid flow,heat and mass transfer in a vertical channel with stretching walls., Int.J.Sci and Innovative Mathematical Res,V.2(10), pp.800-810(2014)
21. Sutton,R.S and Barto,A.G:Exact Navier-stokes solution for pulsatory viscous channel flow with arbitrary pressure gradient., J.Propulsuon and Power,V.24, pp.1412-1424(2008)
22. Shrestha,G.M and R.M.Terril:Laminar flow through parallel and uniformly porous walls of different permeability, ZAMP, V.16,pp.470-482(1965)
23. Shrestha,G.M and R.M.Terril:Laminar flow with large injection through parallel and uniformly porous walls of different permeability,Quart.J.Mech and Appl.Mech., V.21, pp.413-432(1968)
24. Taylor,C.L ,Banks,W.H.H , Zaturaska,M.B and Drazin,P.G:Three dimensional flow in porous channel., Quart. J.Mech.Appl., V.44, pp.105-133(1991)
25. Terrill,R.M:Laminar flow in a uniformly porous channel with large injection., Aeronaut. Q.,V.15,pp. 299-310(1965)
26. Wang,C.Y:Analysis of viscous flow due to a stretching sheet with surface slip and suction,J.Nonlinear Analysis.Real World Applications,V.10,pp.375-380(2009).
27. Watson,E.B and Banks,W.H.H, Zaturaska, M.B and Drazen,F.G: On transition to chaos in two dimensional channel flow symmetrically driven by accelerating walls., J.Fluid Mech.,V.212,pp.451-485 (1990)
28. Xinhui Si, Liancum Zheng, Ping Lin, Xinxin Zhang,Yan Zhang: Flow and heat transfer of a micropolar fluid in a porous channel with expanding or Contracting wall, Int.J.Heat and Mass transfer, V.67, pp.885-895(2013)
29. Zheng,L,Zhao,N and Zhang,X: Asymptotic solutions for laminar flow in a channel with uniformly accelerating rigid porous walls.,J.University of Sci and Technology Bei jeing.

**Source of support: Nil, Conflict of interest: None Declared.**

**[Copy right © 2018. This is an Open Access article distributed under the terms of the International Journal of Mathematical Archive (IJMA), which permits unrestricted use, distribution, and reproduction in any medium, provided the original work is properly cited.]**